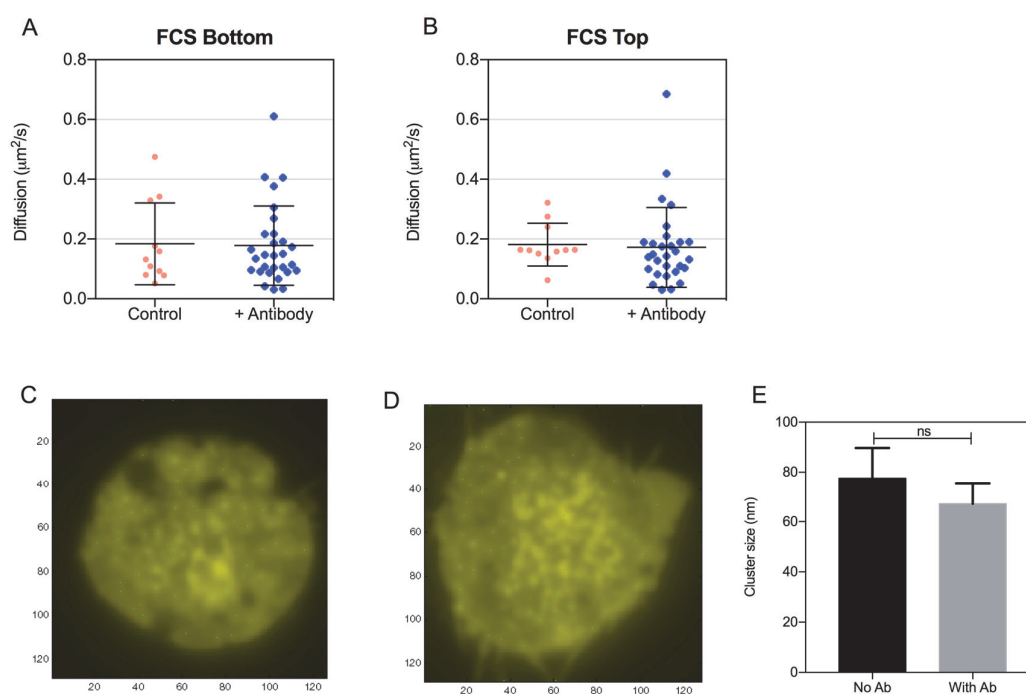


## SUPPLEMENTARY MATERIALS

### Supplementary Figures



**Fig. S1: Diffusion rate and cluster size at the cell surface are not affected by antibody binding.**

Diffusion detected by FCS of YFP-tagged HLA-B51 in the 721.221 cell line. The movement of YFP was measured without antibody (Control) or labeled with an antibody recognizing the YFP-tagged HLA (+Antibody). (A) HLA-B51-YFP diffusion coefficient, measured on the bottom of the cell. (B) B51-YFP, measured on the top of the cell. Data was merged from two to four independent experiments, 11–29 cells per group. No statistically significant differences were detected (Mann-Whitney nonparametric test). (C, D) Ly49A-GFP in unlabelled CHO cells (C) or in CHO cells labelled with an antibody that recognizes Ly49A (clone JR9.318) coupled to Alexa594 (E) Cluster size quantification of Ly49A-GFP without antibody added (No Ab) or Ly49A-GFP detected by anti-Ly49A antibody as in D (With Ab). Quantification was made with a home-written script in Matlab, defining cluster size at half the intensity of max intensity for each cluster (full width half maximum). Identified cluster maxima are marked by a small bright dot (one pixel) in C and D.

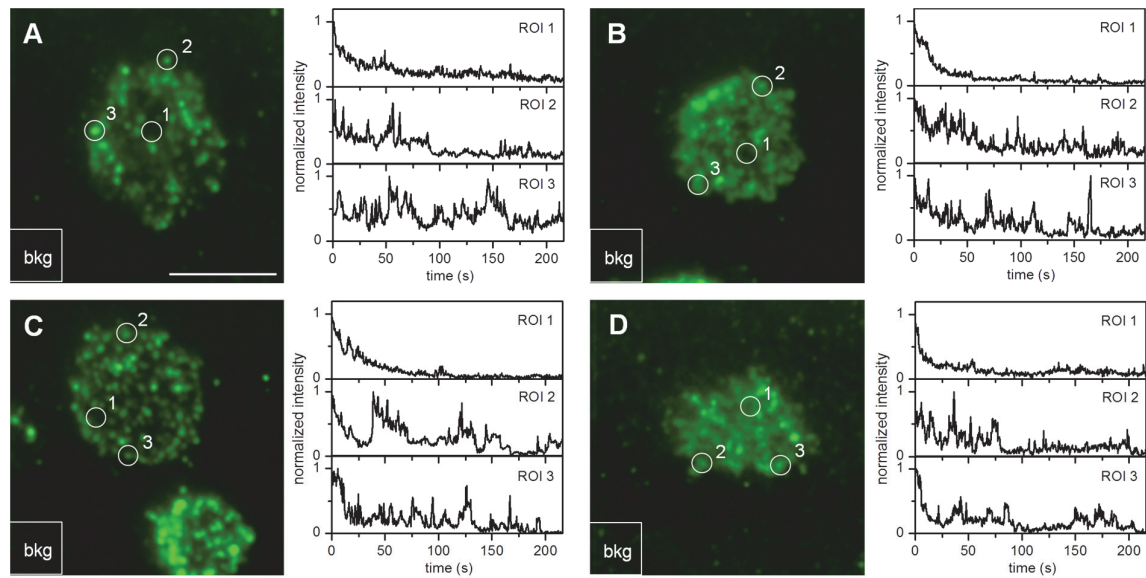


**Fig. S2. Dynamic clustering of NKp46 and Ly49A at the NK cell surface.**

Representative fluorescence images of (A) NKp46 (MFP488 fluorophore) and (B) Ly49A (YE1/48 clone, FITC fluorophore) in freshly isolated NK cells from *MHC<sup>-/-</sup>* mice. (C) NKp46 and (D) Ly49A in NK cells from *H-2D<sup>d</sup>* mice detected with the same antibodies. The images are merged from 6000 frames acquired at a rate of 36 ms frame to frame rate. Scale bar, 5  $\mu\text{m}$ . To the right of each image, the fluorescence intensity traces of three representative regions, indicated by white circles numbered 1-3, are shown. Trace 1 show a region without accumulated fluorescence, and traces 2-3 show clusters of high intensity. The latter show that fluorescent fluctuations occur throughout the time series in these spots, indicating transient confinement periods of receptors or receptor clusters. From each trace, the background (bkg, white box) was subtracted.

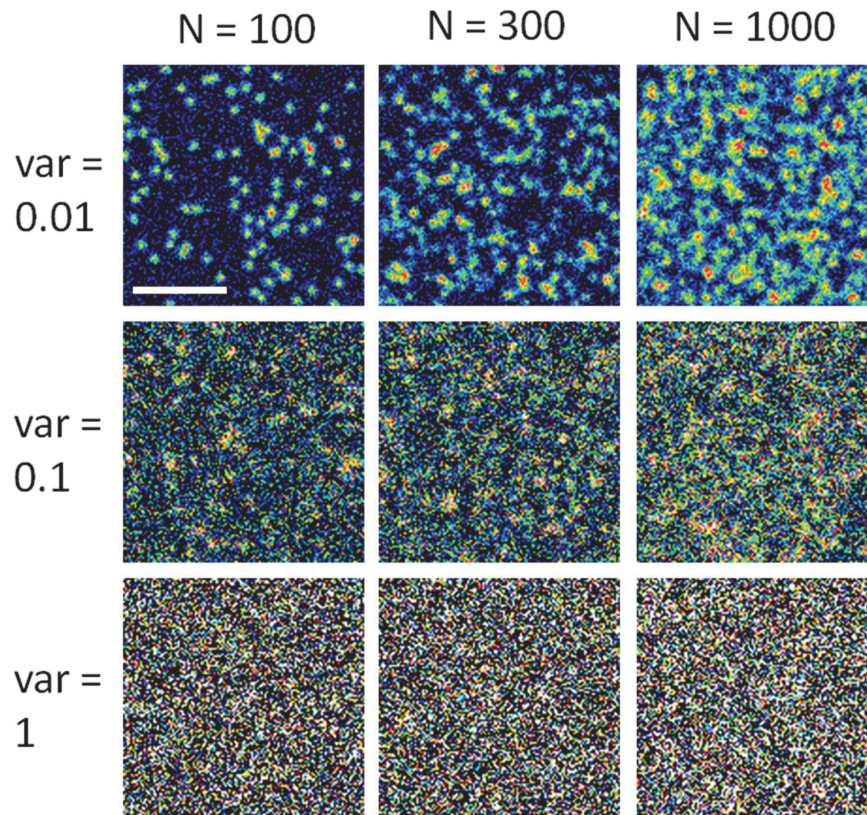


**Fig. S3 Simulation of diffusion with different numbers of molecules and variance of the noise.**

Regions of interest from the simulated data, showing different number of molecules in the different columns and different variance of the noise in the rows. Scale bar, 5  $\mu\text{m}$ .

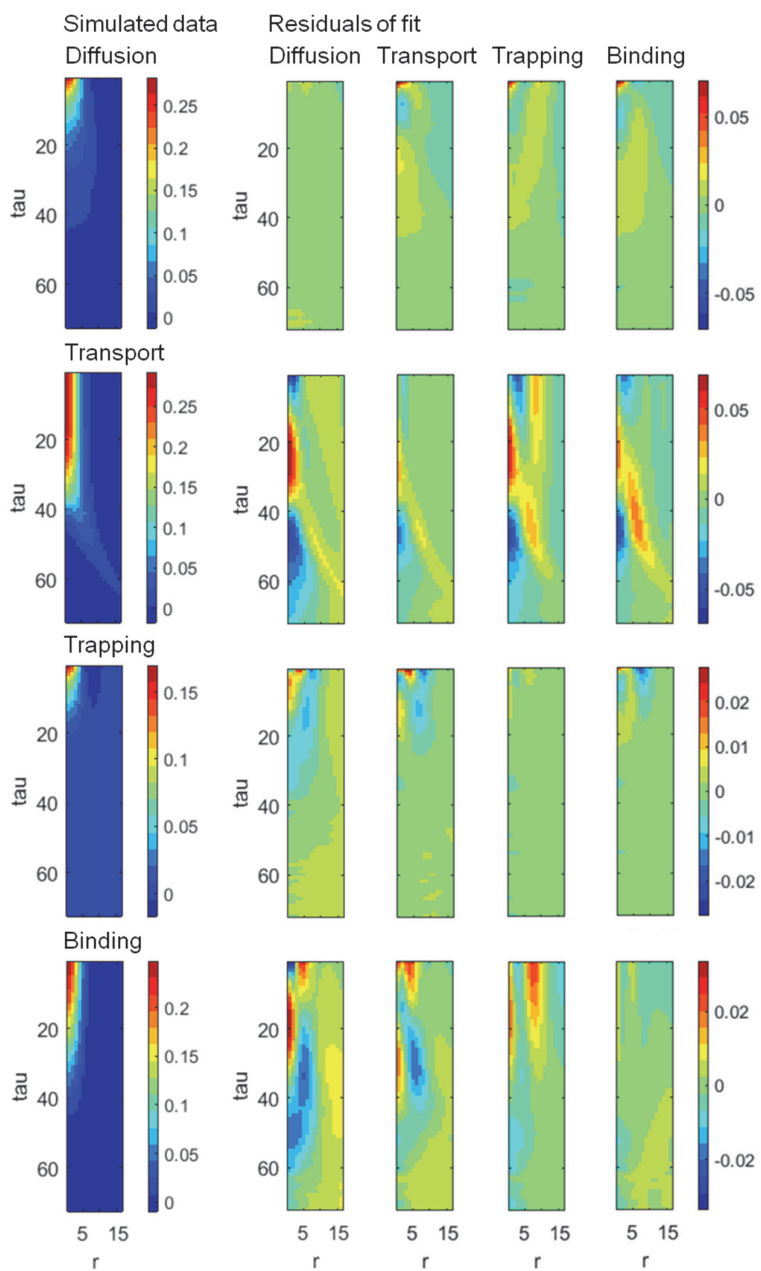


**Fig. S4. Fitting of simulated data sets of the different modes of movement.**

One thousand molecules exhibiting different modes of dynamics were simulated as described in the Materials & Methods and then fitted to the same four models of movement as the biological data. The left column of panes shows the simulated data of the different modes of movement, and the four columns to the right show the residuals when each simulated data set was fitted to the respective models. The  $R^2$  values of each fit is given in Supplementary Table 2.

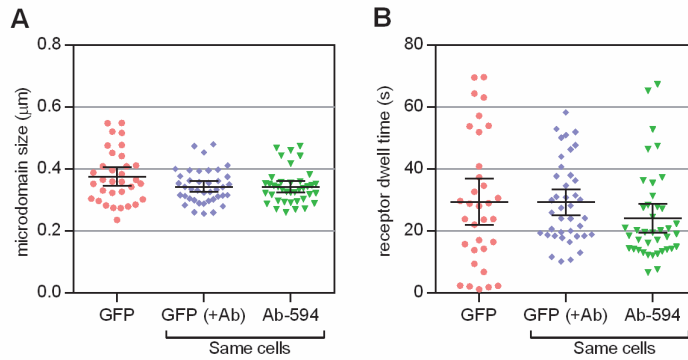


**Fig. S5: Cluster dynamics of transfected Ly49A-GFP at the cell surface is not significantly affected by antibody binding.**

iMSD carpet analysis of binding time of Ly49A in Ly49A-GFP-expressing CHO AA8 cells  
**(A)** Microdomain size. **(B)** Receptor dwell time. X-axis labels: GFP = Ly49A-GFP in cells without antibody labelling; GFP (+Ab) = Ly49A-GFP measured in cells where Ly49A was labeled with antibody; Ab-594 = Measurement of the antibody fluorescence in the same dually labelled cells. Data merged from three independent experiments, 34–40 cells per group. No statistically significant differences between groups, as tested by Kruskal Wallis nonparametric test with Dunn's multiple comparison correction.

## Ly49A Actin alterations

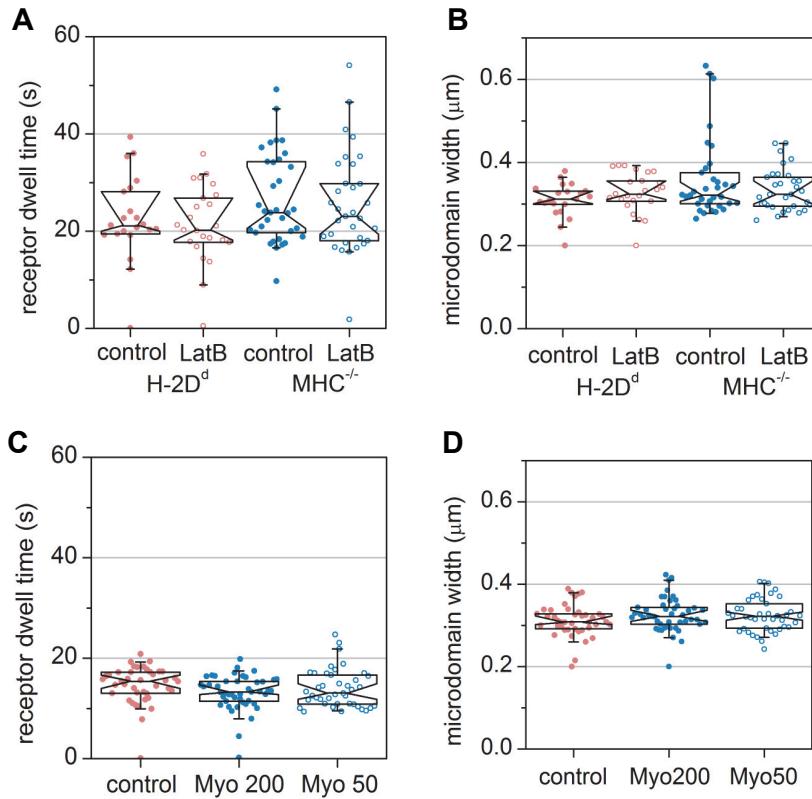


**Fig. S6: Carpet iMSD analysis of Ly49A after LatB and Myovin1 treatment.**

Neither of the treatments affected the receptor dwell time of Ly49A or the width of Ly49A microdomains, as detected by antibody (clone JR9.318 labeled with Abberior star 635). (A, C) Receptor dwell time (B, D) Microdomain size. X-axis labels: control= no treatment, LatB = Latrunculin B treatment, Myo 200 = 200  $\mu\text{g}/\text{ml}$  Myovin1, Myo50 = 50  $\mu\text{g}/\text{ml}$  Myovin 1, in *H-2D<sup>d</sup>* cells. Lat B data was merged from three independent experiments, 22–34 cells per group. Myosin data was merged from three independent experiments, 41–47 cells per group). No statistically significant differences between groups, as tested by Kruskal-Wallis nonparametric test with Dunn's multiple comparison correction.

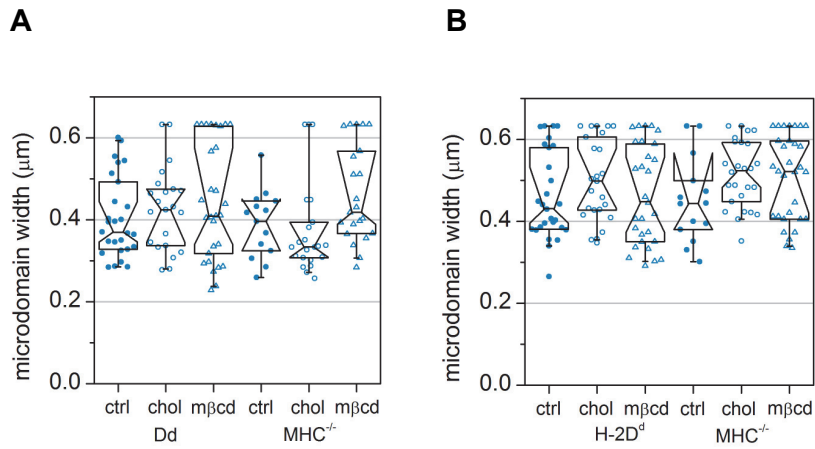


**Fig. S7. Width of NKp46 and Ly49A microdomains after cholesterol and M $\beta$ CD treatment.**

Treatment with cholesterol (chol) or methyl- $\beta$ -cyclodextrin (M $\beta$ CD) had no effect on the width of NKp46 or Ly49A microdomains as detected by antibodies recognizing each receptor. Fluorophores: Anti-NKp46-MFP-488 and anti-Ly49A (clone JR9.318): Abberior star 635. Each dot represents one cell. N= 27 *H-2D<sup>d</sup>* Ctrl, 21 *H-2D<sup>d</sup>* Chol, 29 *H-2D<sup>d</sup>* M $\beta$ CD, and 14 *MHC<sup>-/-</sup>* ctrl, 21 *MHC<sup>-/-</sup>* Chol, 21 *MHC<sup>-/-</sup>* M $\beta$ CD (A); N=27 *H-2D<sup>d</sup>* ctrl, 24 *H-2D<sup>d</sup>* Chol, 28 *H-2D<sup>d</sup>* M $\beta$ CD, and 14 *MHC<sup>-/-</sup>* ctrl, 23 *MHC<sup>-/-</sup>* Chol, 25 *MHC<sup>-/-</sup>* M $\beta$ CD (B). Data were pooled from six independent experiments.

## Supplementary Tables

**Table S1. Simulation of diffusion with different numbers of molecules,  $N$ , and variance,  $Var$ , of the noise.**

Least-squares fitted results of the four different models to the simulated data of Supplementary Fig. 3. In each case, the diffusion model gave the best fit to the simulated data.

Simulation Parameters		$R^2$ Values of Fitted Models			
$N$	$Var$	Diffusion	Transport	Trapping	Binding
100	0.01	0.99	0.96	0.93	0.95
300	0.01	0.99	0.95	0.95	0.95
1,000	0.01	0.99	0.96	0.97	0.95
100	0.1	0.99	0.96	0.97	0.95
300	0.1	0.99	0.96	0.98	0.96
1,000	0.1	0.99	0.96	0.98	0.96
100	1	0.99	0.95	0.96	0.95
300	1	0.99	0.95	0.97	0.95
1,000	1	0.99	0.95	0.97	0.95



**Table S2. R<sup>2</sup> of fitting simulated data to the four different models, using carpet iMSD analysis.**

In the high signal to noise ratio simulations, the noise variance was 0,01 and in the low signal to noise ratio the noise ratio was 1. The highest R<sup>2</sup> for each model are marked with bold text and yellow background color.

Simulated Data	Fitted Model			
	Diffusion	Transport	Trapping	Binding
High signal to noise ration				
Diffusion	<b>0,994</b>	0,953	0,964	0,948
Transport	0,933	<b>0,987</b>	0,937	0,959
Trapping	0,929	0,953	<b>0,997</b>	0,978
Binding	0,951	0,977	0,978	<b>0,996</b>
Low signal to noise ratio				
diffusion	<b>0,99</b>	0,95	0,97	0,95
transport	0,92	<b>0,98</b>	0,94	0,96
trapping	0,92	0,94	<b>0,99</b>	0,97
confinement	0,95	0,97	0,97	<b>0,99</b>

**Table S3. Median R<sup>2</sup> and percentage of cells with best fit for each model.**

The data show the results of fitting the data set shown in Fig 3 D-I to the four different models. The best fit is defined as the highest R<sup>2</sup>. The highest R<sup>2</sup> and the highest percentage of cells with best fit for each model are marked with bold text and yellow background color.

	NKp46		Ly49A (YE1/48)		Ly49A (JR9)	
	H-2D <sup>d</sup>	MHC <sup>-/-</sup>	H-2D <sup>d</sup>	MHC <sup>-/-</sup>	H-2D <sup>d</sup>	MHC <sup>-/-</sup>
<b>median R<sup>2</sup></b>						
Diffusion	0,979	0,981	0,973	<b>0,972</b>	0,984	0,980
Transport	0,968	0,968	0,951	0,949	0,976	0,971
Trapped	0,959	0,960	0,959	0,969	0,968	0,960
Confined	<b>0,984</b>	<b>0,983</b>	<b>0,974</b>	0,970	<b>0,988</b>	<b>0,983</b>
<b>% cells with best fit</b>						
Diffusion	23,5	29,9	48,6	<b>56,8</b>	13,0	26,5
Transport	0,0	0,0	0,0	0,0	0,0	0,0
Trapped	0,0	0,0	0,0	13,5	1,9	0,0
Confined	<b>76,5</b>	<b>70,1</b>	<b>52,9</b>	29,7	<b>85,2</b>	<b>73,5</b>

## **Legends for Supplementary Movies**

### **Movie M1. Single molecule tracking of NKp46 in H-2D<sup>2</sup>.**

Movie of single-molecule trajectories of NKp46 in a freshly isolated *H-2D<sup>d</sup>* NK cell captured at a 20 ms acquisition time. Five consecutive frames were merged to increase the signal to noise ratio. The total length of the movie is 300 (merged) frames.

### **Movie M2. Single molecule tracking of Ly49A in H-2D<sup>2</sup>.**

Movie of single-molecule trajectories of Ly49A in a freshly isolated *H-2D<sup>d</sup>* NK cell captured at a 20 ms acquisition time. Five consecutive frames were merged to increase the signal to noise ratio. The total length of the movie is 300 (merged) frames.